



ISSN: 2617-6548

URL: www.ijirss.com



Lyapunov-based stability analysis of quantum sliding mode controller

Youcef Malek¹, Nadjat Zioui^{2*}, Mohamed Tadjine¹

¹*École Nationale Polytechnique, 10 Rue des Frères OUDEK, El Harrach 16200, Algiers, Algeria.*

²*Université du Québec à Trois-Rivières, 3351 Bd des Forges, Trois-Rivières, QC G8Z 4M3, Canada.*

Corresponding author: Nadjat Zioui (Email: nadjat.zioui@uqtr.ca)

Abstract

This article addresses the lack of formal stability analyses in quantum sliding mode control (QSMC) by providing rigorous proof of stability and convergence based on Lyapunov theory. It also proposes an optimized QSMC approach that reduces quantum resource requirements while preserving control performance. The study begins with a re-evaluation of the conventional QSMC formulation, which implements the sign function using three qubits, along with a Hadamard gate and a CCNOT gate. A Lyapunov-based analysis is conducted to formally demonstrate the stability and convergence of the system. Based on this result, an improved QSMC scheme is introduced. The new design replaces the original structure with a quantum sign detector, a measurement process, and a rotation gate, thus reducing the implementation to two qubits. The proposed method is validated by its application to the speed control of a DC motor. The results show that it maintains efficient performance while requiring fewer computing resources. Simulation results support the feasibility of the approach. This work strengthens the theoretical foundations of QSMC and improves its applicability. The optimized version offers a more efficient and scalable solution for implementation on current quantum hardware with limited qubit availability.

Keywords: Lyapunov stability, Quantum computing, Quantum measurement, Quantum rotations, Sliding mode control.

DOI: 10.53894/ijirss.v9i5.11610

Funding: This study received no specific financial support.

History: Received: 23 February 2026 / Revised: 13 April 2026 / Accepted: 17 April 2026 / Published: 4 May 2026

Copyright: © 2026 by the authors. This article is an open access article distributed under the terms and conditions of the Creative Commons Attribution (CC BY) license (<https://creativecommons.org/licenses/by/4.0/>).

Competing Interests: The authors declare that they have no competing interests.

Authors' Contributions: All authors contributed equally to the conception and design of the study. All authors have read and agreed to the published version of the manuscript.

Transparency: The authors confirm that the manuscript is an honest, accurate, and transparent account of the study; that no vital features of the study have been omitted; and that any discrepancies from the study as planned have been explained. This study followed all ethical practices during writing.

Publisher: Innovative Research Publishing

1. Introduction

Sliding mode control is one of the most popular robust controllers in control theory that has found applications in several fields of engineering such as motors control [1-3] robotic manipulation [4, 5] quadcopters [6-8] aircrafts [9, 10] and spacecrafts [11] as well as underwater vehicles [12-14] among many other applications [15]. The successful integration of this technique went beyond its classical version by introducing higher order versions to reduce chattering issues such as super-twisting and second-order SMC [16, 17] along with adaptive SMC versions [18-21] including adaptive gain options [22]. Thanks to SMC success, sliding mode observers have also gained popularity with the use of several advancements

gained in the context of the SMC design [1, 23]. In the meantime, quantum computing has gained high interest in the latest decades, and many applications are finding echo of this paradigm in various fields. More recently, new versions of the SMC based on the principles of quantum computing have been proposed and successfully applied to control DC motors speed [24] and robotic arms trajectory tracking Fazilat and Zioui [25] and Dahassa, et al. [26].

Zioui, et al. [27] introduced for the first time quantum sliding mode controller (QSMC) based on the implementation of the sign function using quantum gates [24]. The proposed method was successfully applied to DC motor drive control and showed as efficient results as the classic SMC with much less switching and control energy consumption. Later, the proposition of a new quantum subtractor and sign detector circuits were built to generate a quantum space vector pulse width modulation (QSVPWM) [28]. This led to the proposition of a more comprehensive full package of the QSMC that was elaborated by Fazilat and Zioui [25] that integrates quantum subtractor to compute the tracking error, proposes a new quantum adder circuit to compute the sliding surface, and a quantum sign detector to implement the sign function, which is the main pillar of the SMC technique design [25].

The core design of the classic SMC relies on the Lyapunov stability criteria, where the sliding surface is defined to ensure the control objectives are achieved. On the other hand, the control signal is built in such a way that the product between the surface and its derivative is always negative which provides an opposite force to the error that constantly drives the controlled system towards its objectives [29-32]. In parallel, the QSMC design is based on the quantum gates and circuit implementation of the sign function that represents the basis of the SMC [24-26, 28].

While the quantum gates expressions are very well known and although the proposed QSMS techniques show high performances and even surpass the classic counterpart in terms of reduction of tracking errors, convergence time, less chattering and even less energy consumption under simulation or experimentation results [24, 25] one gap remains unexplored, namely the demonstration of the Lyapunov stability of the method. In fact, the authors ensure the convergence of the method based on the convergence of classic SM controller by claiming that QSM is a quantum computing based formulation of the SM controller, therefore the stability of QSM is ensured by the stability of the classic SM. However, this must be mathematically demonstrated, rather than experimentally proved, as experimentation cannot guarantee the exploration of all possible cases that might lead or not to instability in some cases.

In this document, rigorous mathematical proof is established to assess the stability of the QSM controller, where the existing design available in the literature is considered. Moreover, a new optimized version of the QSMC is proposed based on an existing quantum detection method with provided proof of stability that reinforces the credibility and applicability of this technique. The proposed method uses less qubit states and reduces the hardware resources which are of high importance considering quantum issues such as error propagation and hardware costs of this early-stage technology. The proposed method is also applied for speed control of a DC motor to demonstrate its applicability.

The reminder of the document is structured such that section 2 will remind the Lyapunov stability of the classic SM controller. This same section will recall the two QSM controller designs. Section 3 will emphasize the stability proof of both existing and proposed QSM controllers with a discussion of the results. The document will be concluded with a fourth and last section that will recall the contribution, findings and potential future directions.

2. Tools and Methods

2.1. Stability of the classic SM controller

The SM controller relies on the definition of a sliding surface S , attracting the state x of the system, or the tracking error e , on the surface, and maintaining the state on the sliding surface. Its core design is based on the Lyapunov stability principle. In fact, for a system given by its state equations expressed in terms of tracking errors (1), the expression of the controller u defined in (2) will ensure the attractiveness (3) and invariance (4) which maintain the tracking error at zero.

$$\dot{e} = f(x) + g(x)u \tag{1}$$

$$u = \frac{1}{g(x)}[-f(x) - K\text{sign}(e)], \quad K > 0 \tag{2}$$

$$\dot{S} < 0 \tag{3}$$

$$\dot{S} = 0 \Rightarrow S = 0 \tag{4}$$

Since the sliding surface S is selected to ensure the achievement of the control objectives, which are usually the reduction of the tracking error to zero, the convergence of the state towards the sliding error will mean the convergence of the tracking error towards zero. Equation 3 is the core of the stability principle in the sense of Lyapunov convergence, which ensures the stability of the SM controller.

2.2. Brief recall on the quantum computing principles

2.2.1. The Qubit

A qubit is the unit of information in quantum computing. It can hold both logical 0 and 1 values within its state with a probability for each. The following expression represents a qubit state [33].

$$|q\rangle = \alpha|0\rangle + \beta|1\rangle \tag{5}$$

α and β are complex coefficients verifying $|\alpha|^2 + |\beta|^2 = 1$. They can be perceived as the projection of $|q\rangle$ on the eigenstates $|0\rangle$ and $|1\rangle$ or as the probabilities of $|q\rangle$ to be 0 or 1.

The qubit state can be expressed using vectors such as $|0\rangle \equiv \begin{pmatrix} 1 \\ 0 \end{pmatrix}$, $|1\rangle \equiv \begin{pmatrix} 0 \\ 1 \end{pmatrix}$, and $|q\rangle \equiv \begin{pmatrix} \alpha \\ \beta \end{pmatrix}$. It can also be represented in the Bloch sphere as a vector that can be in any point of the sphere as in Figure 1 [27].

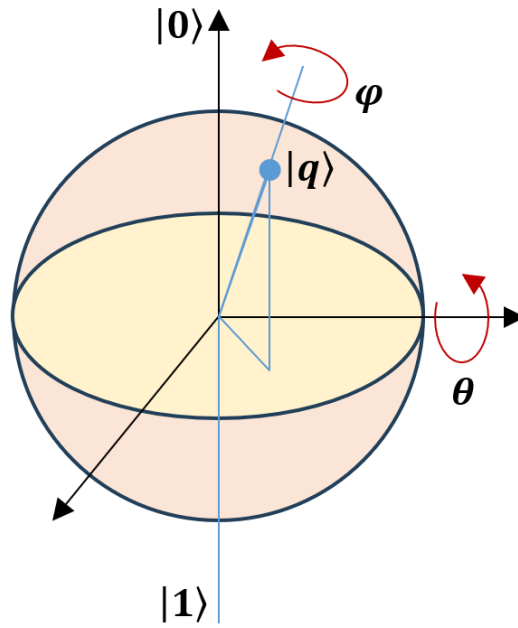


Figure 1.
The Bloch representation of qubit state.

Measuring a qubit state is performed using the inner product. Its objective is to convert the quantum information of a qubit state into classic information 0 or 1. The inner product $\langle 0|q\rangle$ will provide the probability $|\langle 0|q\rangle|^2$ that the qubit state $|q\rangle$ is $|0\rangle$. The inner product $\langle 1|q\rangle$ will provide the probability $|\langle 1|q\rangle|^2$ that the qubit state $|q\rangle$ is $|1\rangle$. Measuring a qubit will collapse it on one of the eigenstates $|0\rangle$ or $|1\rangle$ [33].

2.2.2. One Qubit Operator

A qubit state can be subjected to quantum operators that act on them and change their coefficients, therefore their situation in the Bloch sphere. Among these operators are the identity gate I , the X gate, the Y gate, and the Z gate, known as the Pauli gates [24].

$$I = \begin{pmatrix} 1 & 0 \\ 0 & 1 \end{pmatrix}, X = \begin{pmatrix} 0 & 1 \\ 1 & 0 \end{pmatrix}, Y = \begin{pmatrix} 0 & -i \\ i & 0 \end{pmatrix}, Z = \begin{pmatrix} 1 & 0 \\ 0 & -1 \end{pmatrix} \quad (6)$$

Other quantum operators include the Hadamard gate H and the three quantum rotation gates R_x , R_y , and R_z [24].

$$H = \frac{\sqrt{2}}{2} \begin{pmatrix} 1 & 1 \\ 1 & -1 \end{pmatrix}, R_x = \begin{pmatrix} C\theta & iS\theta \\ iS\theta & C\theta \end{pmatrix}, R_y = \begin{pmatrix} C\theta & S\theta \\ -S\theta & C\theta \end{pmatrix}, R_z = \begin{pmatrix} C\theta & iS\theta \\ iS\theta & -C\theta \end{pmatrix} \quad (7)$$

The quantum operators can be represented by quantum circuits, where operators are denoted by squares and the quantum states by horizontal lines. The quantum circuits are read from left to right and from top to bottom.

2.2.3. Multiple Qubit Operator

There is a possibility of affecting a system of two or more qubits at the same time. For instance, the CNOT gate alters two qubits such that one of the qubits acts as the control bit. The second qubit cannot be shifted unless the control qubit is $|1\rangle$, otherwise, it remains unchanged [24].

The CCNOT gate acts on a system of three qubits. Two of the qubits act as control qubits such as the third qubit is shifted only if both control qubits are in the state $|1\rangle$ [28].

2.3. The Quantum SM Controllers

Quantum SMC (QSMC) is starting to gain popularity in literature and variants are starting to see light. The QSMC core building approach is either based on building the quantum equivalent to the sign function using quantum gates such as Hadamard and CCNOT gates [24] or the use of quantum rotation gates to perform the sign function [25]. In both cases, the proposed solution either considers the remaining operations as oracles to be developed in later works [24] or a complete solution that includes the quantum arithmetic operations for the sliding surface definition as well as the control signal whole expression [25]. However, in both cases, either the quantum rotation gates or Hadamard-CCNOT gates solutions are the core principle of the existing QSMC in the literature.

2.3.1. Case 1

The first approach of building a QSMC is the design of a quantum circuit to mimic the sign function of the expression of the SM controller using basic quantum gates and truth tables, while considering the remaining operations of the

controller's expression as oracles to be lately developed. In their work, Zioui, et al. [27] proposed to implement the sign function QSMC based on the truth Table 1 that defines the quantum circuit behavior.

Table 1.
The quantum sign function logical operation.

Initial states			Final states after quantum circuit		
$ q_3\rangle$	$ q_2\rangle$	$ q_1\rangle$	$ q_3\rangle$	$ q_2\rangle$	$ q_1\rangle$
$ q_3\rangle$	$ 0\rangle$	$ q_1\rangle$	$ 0\rangle$	$ 0\rangle$	$ q_1\rangle$
$ q_3\rangle$	$ 1\rangle$	$ 0\rangle$	$- 1\rangle$	$ 1\rangle$	$ 0\rangle$
$ q_3\rangle$	$ 1\rangle$	$ 1\rangle$	$ 1\rangle$	$ 1\rangle$	$ 1\rangle$

In Table 1, Three qubit states are considered, $|q_2\rangle$ for the presence or not of an error, $|q_1\rangle$ that represents the sign of the error is any, and $|q_3\rangle$ to reproduce the control signal (or the operation of the sign function). The behaviors of the first and second qubits are defined in Table 2. In this design, the sliding surface is the tracking error itself. This means that this approach is valid either for single input single output (SISO) systems or linearized decoupled multi-input multi output (MIMO) systems.

Table 2.
The behavior of the qubits $|q_1\rangle$ and $|q_2\rangle$.

Qubit state $ q_2\rangle$	Qubit state $ q_1\rangle$	Meaning
$ 0\rangle$	$ 0\rangle$ or $ 1\rangle$	The error is zero. $ q_3\rangle$ should be $ 0\rangle$.
$ 1\rangle$	$ 0\rangle$	The error is negative. $ q_3\rangle$ should be $ 1\rangle$.
$ 1\rangle$	$ 1\rangle$	The error is positive. $ q_3\rangle$ should be $- 1\rangle$.

The quantum circuit that replicates the behavior defined in Table 1 can be performed using a Hadamard gate that will equally distribute the coefficients on both eigenstates of the qubit state $|q_1\rangle$ and will make the negative sign appear for one eigenstate coefficient while the other remains positive. Which will make both signs available in the expression of the result. After the Hadamard gate, The CCNOT will be performed to implement the conditional operation of qubit $|q_3\rangle$ that depends both on $|q_1\rangle$ and $|q_2\rangle$ states as in the following. Figure ... depicts the quantum circuit defines in (8).

$$|q_3\rangle = CCNOT(|q_3\rangle, |q_2\rangle, H|q_1\rangle) \tag{8}$$

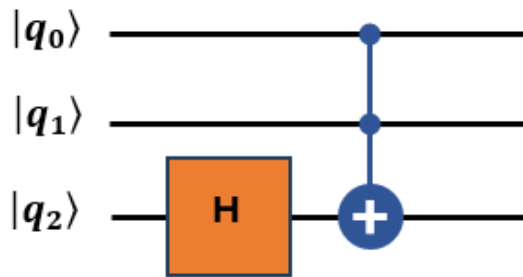


Figure 2.
The quantum circuit of the sign function of the QSM.

2.3.2. Case 2

The second approach of building a QSMC is the design of a quantum circuit of the sign function using the quantum rotation gate R_y through behavior observation. In their work, Zioui, et al. [28] not only proposed to implement the sign function of the QSMC using the R_y quantum rotation gate, but they also introduced the quantum circuits to implement the arithmetic operations that could help implement of full version of the QSMC as it has been established later by Zioui, et al. [28].

The quantum rotation gate R_y based method encodes a number, generally the tracking error or the sliding surface, which sign must be determined, as a qubit state $|q_s\rangle$. This is performed considering the investigated number, or the normalized equivalent of it, to be the component $\cos\theta_s$ of the eigenstate $|0\rangle$ as follows.

$$|q_s\rangle = \cos\theta_s|0\rangle + \sin\theta_s|1\rangle \tag{9}$$

This method needs the use of the Arccosine function, which is considered as an oracle. The use of the Arccosine function will imply that the computed angle θ_s varies between 0 and π , meaning that the investigated number that has been embedded in $\cos\theta_s$ will vary between -1 and $+1$. If the qubit state $|q_s\rangle$ is rotated with $-\frac{\pi}{4}$, then the following stands:

- A variation of θ_s between 0 and $\frac{\pi}{2}$ will lead to a variation of $\theta_s - \frac{\pi}{4}$ between $-\frac{\pi}{4}$ and $+\frac{\pi}{4}$ and a variation of $\cos^2\left(\theta_s - \frac{\pi}{4}\right)$ between 0.5 and 1. This will make the measurement of the state $R_y\left(-\frac{\pi}{4}\right)|q_s\rangle$ equal to $|1\rangle$ and encodes $\cos\theta_s$ as being positive.

- On the other hand, a variation of θ_s between $\frac{\pi}{2}$ and π will lead to a variation of $\theta_s - \frac{\pi}{4}$ between $+\frac{\pi}{4}$ and $+\frac{3\pi}{4}$ and a variation of $\cos^2\left(\theta_s - \frac{\pi}{4}\right)$ between 0 and 0.5. This will make the measurement of the state $R_y\left(-\frac{\pi}{4}\right)|q_s\rangle$ equal to $|0\rangle$, which encodes $\cos\theta_s$ as being negative.

An X gate is then added to inverse the resulting logics. Therefore, if the number investigated is positive, the output will be $|0\rangle$ and if negative, the output will be $|1\rangle$. This will prepare the field for the application of another rotation gate.

With sign detection being established, the proposed implementation of the control signal u can be optimized through the implementation of another y rotation gate with an angle of $+\frac{\pi}{4}$ applied directly to the measured state of $X R_y\left(-\frac{\pi}{4}\right)|q_s\rangle$ which will be collapsed on the eigenstate $|0\rangle$ if $\cos\theta_s$ is positive or $|1\rangle$ if $\cos\theta_s$ is negative.

The quantum circuit of this technique is depicted in Figure 3 and its formula is expressed in the following.

$$|u\rangle = R_y\left(+\frac{\pi}{4}\right)|q_0\rangle \tag{10}$$

$|q_0\rangle$ is the result of the measurement $\langle 0|X R_y\left(-\frac{\pi}{4}\right)|q_s\rangle$ encoded as qubit, or the collapsed state after measurement.

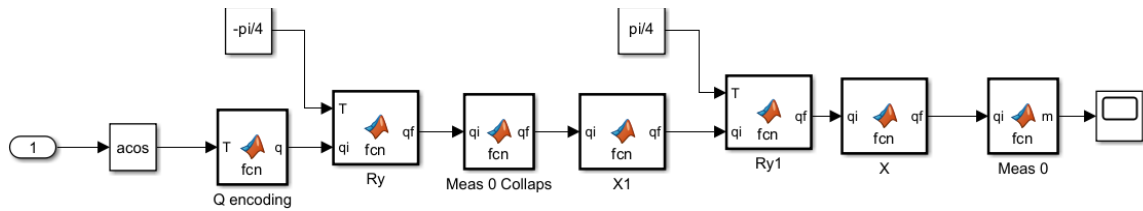


Figure 3.
The implementation of the QSMC using quantum X and rotation gates.

The control signal using this proposed method will be collected on the $|1\rangle$ component of the qubit state $|u\rangle$. The collection of the signal on the $|0\rangle$ component requires additional application of an X gate. Table 3 summarizes the operations of this technique.

Table 3.
Operation of rotations gates based QSMC technique.

Sign of $\cos\theta_s$	$\cos^2\left(\theta_s - \frac{\pi}{4}\right)$	$\langle 0 X R_y\left(-\frac{\pi}{4}\right) q_s\rangle$	$ u\rangle$
$\cos\theta_s > 0$	$0.5 \rightarrow 1$	$ 0\rangle$	$\frac{\sqrt{2}}{2}(0\rangle - 1\rangle)$
$\cos\theta_s \leq 0$	$0 \rightarrow 0.5$	$ 1\rangle$	$\frac{\sqrt{2}}{2}(0\rangle + 1\rangle)$

3. Results and Discussion

3.1. First Case Scenario

Using Tables 1 and 2 the following expressions for the qubits $|q_1\rangle$ and $|q_2\rangle$ will be considered.

$$|q_1\rangle = \begin{pmatrix} C\theta_1 \\ e_{sign} \end{pmatrix} \tag{11}$$

$$|q_2\rangle = \begin{pmatrix} C\theta_2 \\ e_{pres} \end{pmatrix} \tag{12}$$

e_{pres} is a Boolean entity that indicates the presence of an error or not: 0 if the error is zero and 1 if the error is not zero.

e_{sign} is a Boolean entity that indicates the sign of the error: 0 if the error is negative and 1 if the error is positive.

$C\theta_1$ and $C\theta_2$ refer to the cosine of θ_1 and θ_2 , respectively.

To ensure $|q_1\rangle$ and $|q_2\rangle$ are correctly encoded as qubits, the following stands.

$$\theta_1 = \text{Asin}(e_{sign}) \tag{13}$$

$$\theta_2 = \text{Asin}(e_{pres}) \tag{14}$$

The control signal $|q_3\rangle$ is initialized to the eigenstate $|0\rangle$.

The application of the Hadamard gate to $|q_1\rangle$ will result in the following.

$$H|q_1\rangle = \frac{\sqrt{2}}{2} \begin{pmatrix} C\theta_1 + e_{sign} \\ C\theta_1 - e_{sign} \end{pmatrix} \tag{15}$$

And the computation of the CCNOT will provide the following result.

$$CCNOT(|0\rangle, |q_1\rangle, H|q_2\rangle) = \begin{pmatrix} \frac{\sqrt{2}}{2}(C\theta_1 + e_{sign}) C\theta_2 \\ 0 \\ \frac{\sqrt{2}}{2}(C\theta_1 + e_{sign}) e_{pres} \\ 0 \\ \frac{\sqrt{2}}{2}(C\theta_1 - e_{sign}) C\theta_2 \\ 0 \\ \frac{\sqrt{2}}{2}(C\theta_1 - e_{sign}) e_{pres} \\ 0 \end{pmatrix} \quad (16)$$

The expression of the component $|110\rangle$ from (16) is as follows.

$$|110\rangle = \frac{\sqrt{2}}{2}(C\theta_1 - e_{sign}) e_{pres} \quad (17)$$

In this last expression, if the error is positive, then $e_{pres} = 1$ (The error is present: $|q_2\rangle = |1\rangle$) and $C\theta_1 = 0$ with $e_{sign} = 1$ ($|q_1\rangle = |1\rangle$). Therefore, when the error is positive, expression $|110\rangle$ becomes: $|110\rangle = -\frac{\sqrt{2}}{2}$.

Likewise, if the error is negative, $C\theta_1 = 1$ leading to $e_{sign} = 0$ ($|q_1\rangle = |0\rangle$). Considering $e_{pres} = 1$ (The error is present: $|q_2\rangle = |1\rangle$), the expression of the component $|110\rangle$ will be: $|110\rangle = +\frac{\sqrt{2}}{2}$, Which will ensure the product $e_{sign}(e)$ always negative. Therefore, the proposed approach leads to the Lyapunov-based stability of this first case proposed QSMC.

3.2. Second Case Scenario

The development of expression (10) with measurement on the $|0\rangle$ component will result in the following.

$$|u\rangle = X R_y\left(+\frac{\pi}{4}\right) |q_0\rangle = \begin{cases} \frac{\sqrt{2}}{2} \begin{pmatrix} 0 & 1 \\ 1 & 0 \end{pmatrix} \begin{pmatrix} 1 & 1 \\ -1 & 1 \end{pmatrix} \begin{pmatrix} 1 \\ 0 \end{pmatrix} = \frac{\sqrt{2}}{2} \begin{pmatrix} -1 \\ 1 \end{pmatrix} & \text{if } \cos\theta_s > 0 \\ \frac{\sqrt{2}}{2} \begin{pmatrix} 0 & 1 \\ 1 & 0 \end{pmatrix} \begin{pmatrix} 1 & 1 \\ -1 & 1 \end{pmatrix} \begin{pmatrix} 0 \\ 1 \end{pmatrix} = \frac{\sqrt{2}}{2} \begin{pmatrix} 1 \\ 1 \end{pmatrix} & \text{if } \cos\theta_s \leq 0 \end{cases} \quad (18)$$

Collecting the control signal u on the $|0\rangle$ component of qubit $|u\rangle$ will result in $u = -\frac{\sqrt{2}}{2}$ if $\cos\theta_s$ is positive and $u = +\frac{\sqrt{2}}{2}$ if $\cos\theta_s$ is negative. In this case, the controller generates a restoring force proportional to the error and in the opposite direction, guaranteeing Lyapunov asymptotic stability.

3.3. Application Case

The control of a DC motor is considered as application for the proposed method. The DC motor's characteristics are summarized in Table 4. The model of the motor is provided in (19) and the controller in (20). Figure 4 depicts the model of the motor using Simulink MATLAB.

$$\begin{cases} \frac{d\omega}{dt} = \frac{K_a}{J} i_a - \frac{B_m}{J} \omega \\ \frac{di_a}{dt} = -\frac{R_a}{L_a} i_a - \frac{K_b}{L_a} \omega + \frac{1}{L_a} u \end{cases} \quad (19)$$

ω is the angular speed of the rotor in rad/s.

i_a is the current of the motor in A.

u is the voltage of the motor in V.

K_a is the torque constant in N.m/A.

K_b is the speed constant in N.m.s.

J is the inertia constant in kg.m².

R_a is the resistance of the rotor in Ω .

L_a is the inductance of the rotor in H.

$$u = R_a i_a + K_b \omega + \frac{L_a B_m}{K_a} \frac{d\omega}{dt} + \frac{J}{K_a} \frac{d^2\omega_r}{dt^2} - \frac{J}{K_a} K_\omega \frac{de_\omega}{dt} - \frac{JK_s}{K_a} \text{sign}(S) \quad (20)$$

$e_\omega = \omega - \omega_r$ is the tracking error for the motor's speed in rad/s.

K_s and K_ω are positive constants determined to impose a convergence dynamic for the speed. The constant K_ω should be higher than K_s to ensure the correct convergence of the dynamics.

S is the sliding surface defined by $S = \frac{de_\omega}{dt} + K_\omega e_\omega$.

The application of the controller defined in (20) to the system will lead to the dynamics in (21) that verifies both attractivity and invariance, therefore, the Lyapunov stability of the system.

$$\frac{dS}{dt} = -K_s \text{sign}(S) \quad (21)$$

The QSMC controller is derived from expression (20) with replacement of $\text{sign}(e_\omega)$ by $X R_y\left(+\frac{\pi}{4}\right) |q_0\rangle$. Such as $|q_0\rangle$ is the collapsed quantum state after measuring $\left\langle 0 \left| X R_y\left(-\frac{\pi}{4}\right) |q_s\rangle \right\rangle$, where $|q_s\rangle$ is the qubit encoding of the error e_ω .

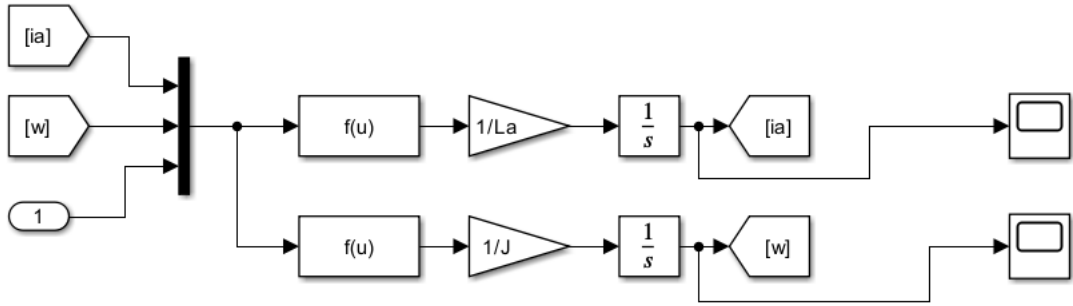
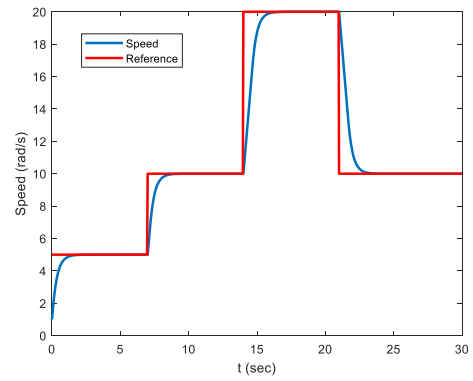
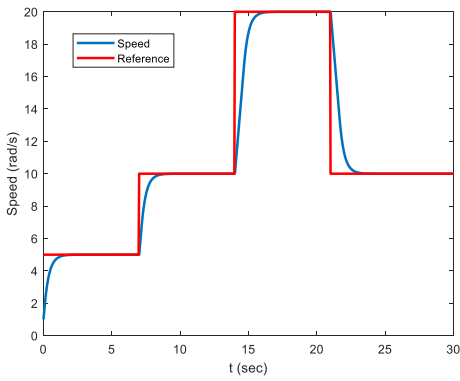


Figure 4.
The DC motor Simulink model.

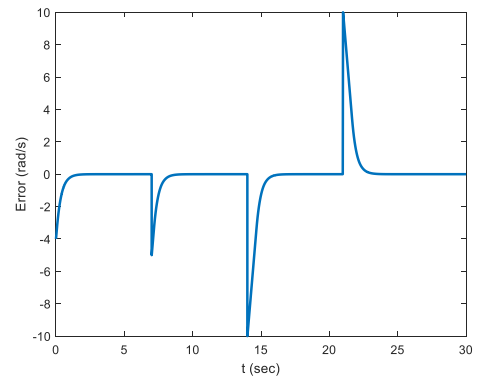
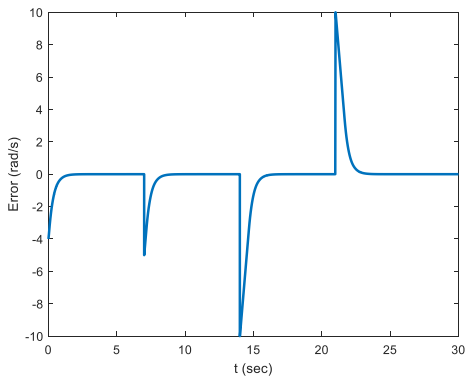
Figure 5 illustrates the tracking performances of the motor's speed using classic and quantum SMC. Figures 6 and 7 represent the tracking errors and control signals, respectively.



(a)

(b)

Figure 5.
Speed results: (a) using QSCM, (b) using classic SMC.



(a)

(b)

Figure 6.
Tracking speed error: (a) using QSCM, (b) using classic SMC.

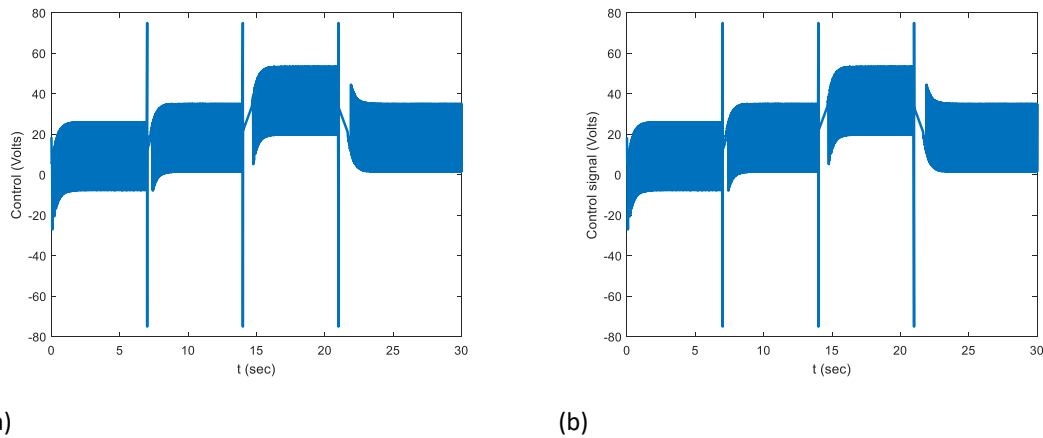


Figure 7.
Control signal: (a) using QSCM, (b) using classic SMC.

3.4. Discussion

Figure 5 demonstrates strong tracking performance for both the classical SMC and the proposed QSMC. The tracking errors shown in Figure 6 indicate that both approaches achieve equivalent speed-control precision. The control signals exhibit nearly identical profiles, further confirming the effectiveness of the proposed QSMC. Analysis of the energy signals also corroborates these results.

It is important to note, however, that the classical approach requires multiple classical bits to perform information encoding and arithmetic operations, whereas the quantum implementation relies on only two qubits with appropriate error encoding and basic quantum spin operations.

This represents a significant advancement in the application of quantum computing to practical engineering problems, paving the way for turnkey solutions that can be deployed on real quantum hardware.

4. Conclusion

This work establishes a formal stability proof for the quantum sliding mode controller (QSMC), a control strategy that has recently gained increasing attention in the scientific literature. Although the method has already been applied in several engineering contexts, no rigorous and explicit stability analysis had been reported prior to this study. In addition, a novel QSMC approach is proposed. Lyapunov-based stability is successfully demonstrated for both the existing and the proposed controllers, providing a solid theoretical foundation and enhancing the credibility of QSMC for future research and practical applications.

Future research may explore additional QSMC formulations beyond the two approaches investigated in this work, as well as more efficient quantum computing-based strategies aimed at reducing sliding mode control chattering. Further directions include the implementation and experimental validation of these methods on real quantum hardware as it becomes available.

References

- [1] R. Zu, M. Li, Z. Huang, Y. Huang, and D. Xu, "Fast terminal integral sliding mode disturbance observer-based sliding mode current control for SPMSM systems," *Journal of Power Electronics*, vol. 26, no. 1, pp. 101-115, 2026, <https://doi.org/10.1007/s43236-025-01212-0>.
- [2] G. Qin, M. Wang, G. Cao, Q. Wang, and Y. Liao, "PID sliding mode control of PMSM based on improved terminal sliding mode reaching law," *Energies*, vol. 18, no. 10, p. 2661, 2025, <https://doi.org/10.3390/en18102661>.
- [3] D. Shi, R. Hou, D. Gerada, C. Hua, Y. Wang, and Y. Ji, "PMSM control via composite logarithmic sliding mode control," *IET Electric Power Applications*, vol. 19, no. 1, p. e70122, 2025, <https://doi.org/10.1049/elp2.70122>.
- [4] H. D. Long, "Observer-based finite-time adaptive reinforced super-twisting sliding mode control for robotic manipulators," *Advanced Engineering Research (Rostov-on-Don)*, vol. 25, no. 4, pp. 337-349, 2025, <https://doi.org/10.23947/2687-1653-2025-25-4-2209>.
- [5] M. H. Nguyen and T. T. K. Nguyen, "A method integral sliding mode control to minimize chattering in sliding mode control of robot manipulator," *International Journal of Robotics and Automation*, vol. 14, no. 4, pp. 345-355, 2025.
- [6] S. Kumar and L. Dewan, "Path following control for quadcopters with super twisting sliding mode control with PID sliding surface technique," *Proceedings of the Institution of Mechanical Engineers, Part G: Journal of Aerospace Engineering*, vol. 240, no. 3, pp. 530-542, 2026.
- [7] P. A. Darwito *et al.*, "Indoor quadcopter localization using fuzzy-sliding mode control for robust navigation," *International Journal of Robotics & Control Systems*, vol. 5, no. 3, 2025, <https://doi.org/10.31763/ijrcs.v5i3.1941>.
- [8] A. Yesmin and A. Sinha, "Sliding mode controller for quadcopter UAVs: A comprehensive survey," *Drones*, vol. 9, no. 9, p. 625, 2025, <https://doi.org/10.3390/drones9090625>.
- [9] Y. Yuqi, L. Siyuan, and Z. Di, "Adaptive sliding mode model-free control for aircraft attitude control with system uncertainty," *Advances in Astronautics*, vol. 8, no. 3, pp. 257-272, 2025, <https://doi.org/10.1007/s42423-025-00171-9>.
- [10] Y. Ji, P. Li, Y. Lin, Y. Song, Q. Gao, and J. Liu, "Predefined time attitude control of aircraft based on predefined time sliding mode control," *Proceedings of the Institution of Mechanical Engineers, Part I: Journal of Systems and Control Engineering*, vol. 239, no. 2, pp. 247-259, 2025, <https://doi.org/10.1177/09596518241273990>.

- [11] V. Sorochinskii, S. Khoroshylov, I. Levchuk, T. Dubovyk, H. Huz, and O. Romanchuk, "On-off spacecraft relative control in sliding mode via reinforcement learning," *Technical Mechanics*, no. 4, pp. 77-92, 2025.
- [12] F. Wang and L. Wang, "A nonsingular fast terminal sliding mode control for autonomous underwater vehicle," *Journal of Intelligent Manufacturing and Special Equipment*, vol. 7, no. 1, pp. 75-88, 2026, <https://doi.org/10.1108/JIMSE-07-2025-0016>.
- [13] S. Afshari, A. Chatraei, and A. Chatraei, "Adaptive sliding mode fractional-order control of autonomous underwater vehicles," *Asian Journal of Control*, 2025, <https://doi.org/10.1002/asjc.70006>.
- [14] L. Wang, Q. Wang, S. An, P. Liu, and L. Xu, "Free will arbitrary time sliding mode control of autonomous underwater vehicle with external disturbances," *Measurement Science and Technology*, vol. 36, no. 7, p. 076212, 2025.
- [15] A. A. Uppal, M. R. Azam, and J. Iqbal, "Sliding mode control in dynamic systems," *MDPI*, vol. 12, no. 13, p. 2970, 2023, <https://doi.org/10.3390/electronics12132970>.
- [16] Y. Zhang and C. Qian, "Super-twisting algorithm sliding mode control of flexible manipulators considering uncertainty," *Applied Sciences*, vol. 16, no. 1, p. 387, 2025.
- [17] H. D. Le and T. Nestorović, "Second-order nonsingular terminal sliding mode control for tracking and stabilization of cart-inverted pendulum," *Machines*, vol. 14, no. 1, p. 111, 2026, <https://doi.org/10.3390/machines14010111>.
- [18] J. Em-Udom and K. Amnatchotiphan, "An adaptive sliding mode control with integral sliding surface for 3DOF SCARA manipulators," *Engineering, Technology & Applied Science Research*, vol. 15, no. 3, pp. 22445-22451, 2025, <https://doi.org/10.48084/etasr.10269>.
- [19] M. Zhang, Y. Zhu, J. Feng, J. Zhang, and Z. Liu, "Adaptive sliding mode control for load-mapped robotic joint modules with enhanced disturbance rejection," *IEEE Transactions on Industrial Electronics*, vol. 73, no. 5, pp. 7261-7272, 2026.
- [20] O. Geylani and B. Ata, "Experimental validation of adaptive control approaches with terminal and fast terminal sliding mode controls on a nonlinear system," *Arabian Journal for Science and Engineering*, vol. 51, no. 5, pp. 6919-6933, 2026, <https://doi.org/10.1007/s13369-025-10849-9>.
- [21] W. Cao, B. Chai, J. Qiao, T. Wang, and Y. Zhu, "Double-loop adaptive sliding mode control of flexible manipulator based on disturbance observer," *Journal of Vibration and Control*, Jan, 2026, <https://doi.org/10.1177/10775463251407533>.
- [22] Y. Zhang and Y. Li, "Motor automation speed regulation method with sliding mode control and adaptive gain," *Frontiers in Mechanical Engineering*, vol. 11, p. 1715466, 2025, <https://doi.org/10.3389/fmech.2025.1715466>.
- [23] P. N. Tân, H. Đ. S. Tiên, and P. T. Tùng, "Robust sliding mode control based on a new Quasi-sliding mode and adaptive artificial neural networks observer for robot," *Journal of Military Science and Technology*, vol. 108, pp. 21-30, 2025, <https://doi.org/10.54939/1859-1043.j.mst.208.2025.21-30>.
- [24] N. Zioui, A. Mahmoudi, and M. Tadjine, "Developing and implementing a quantum algorithm for the sliding mode controller using multiple qubit operators: Application to DC motor speed drive," *Applied Science and Engineering Progress*, vol. 17, no. 2, pp. 7016-7016, 2024.
- [25] M. Fazilat and N. Zioui, "Quantum-inspired sliding-mode control to enhance the precision and energy efficiency of an articulated industrial robotic arm," *Robotics*, vol. 14, no. 2, p. 14, 2025, <https://doi.org/10.3390/robotics14020014>.
- [26] M. S. Dahassa, M. Fazilat, and N. Zioui, "A novel sliding mode control based on qubit rotation angle for efficient manipulation of robotic arms," *Progress in Engineering Science*, p. 100137, 2025, <https://doi.org/10.1016/j.pes.2025.100137>.
- [27] N. Zioui, A. Mahmoudi, and M. Tadjine, "Representing quantum spins in different coordinate systems for modelling rigid body orientation," *Karbala International Journal of Modern Science*, vol. 9, no. 3, p. 11, 2023, <https://doi.org/10.33640/2405-609X.3313>.
- [28] N. Zioui, A. Mahmoudi, M. Fazilat, O. Kone, D. Reda, and M. Tadjine, "Quantum space vector pulse width modulation for speed control of permanent magnet synchronous machines," *e-Prime-Advances in Electrical Engineering, Electronics and Energy*, p. 101074, 2025, <https://doi.org/10.1016/j.prime.2025.101074>.
- [29] M. Kchaou, M. S. Ali, R. Abbassi, and H. Jerbi, "Analysis and optimization of secure sliding mode observer-based control in nonlinear descriptor systems under attacks," *IEEE Transactions on Cybernetics*, 2026, <https://doi.org/10.1109/TCYB.2026.3651677>.
- [30] M. Al Quran, A. Al-Sheyyab, M. Rawashdeh, and A. rahman Alheyasat, "An integrated sliding mode and lyapunov-based control approach for robust quadcopter trajectory tracking," *Journal of Engineering and Technological Sciences*, vol. 58, no. 2, pp. 257-273, 2026, <https://doi.org/10.5614/j.eng.technol.sci.2026.58.2.8>.
- [31] H. Chaabane, K. D. Eddine, C. Salim, and H. Djamel, "Speed sensorless vector control of double star induction machine using sliding mode observer based Lyapunov stability," *Model. Meas. Control A*, vol. 94, no. 1-4, pp. 1-7, 2021.
- [32] T. Diaby, M. A. Zohdy, and A. Shaout, "A robust and adaptive Lyapunov-sliding mode control strategy for electric motor applications," *Transactions on Machine Learning and Artificial Intelligence*, vol. 13, no. 6, pp. 24-39, 2025.
- [33] A. Adedoyin *et al.*, "Quantum algorithm implementations for beginners," *arXiv preprint arXiv:1804.03719*, 2018, <https://doi.org/10.48550/arXiv.1804.03719>.